Available online at www.sciencedirect.com
ScienceDirect
Journal of Sound and Vibration 311 (2008) 1141–1160
JOURNAL OF SOUND AND VIBRATION
www.elsevier.com/locate/jsvi

Multi-objective optimization of seismically isolated high-rise building structures using genetic algorithms

S. Pourzeynali*, M. Zarif

Department of Civil Engineering, Faculty of Engineering, The University of Guilan, Rasht, I.R. Iran

Received 11 July 2006; received in revised form 30 August 2007; accepted 3 October 2007
Available online 26 November 2007

Abstract

In this paper, suppression of the dynamic response of tall buildings, supported on elastomeric bearings with both linear and nonlinear behaviors, is studied. The isolated building is modeled as a shear-type structure having one lateral degree of freedom at each story level. The elastic supports are modeled as an additional degree of freedom having three unknown parameters: mass, stiffness, and damping ratio. The main objective of the paper is to find the optimal values of the parameters of the base isolation system, using genetic algorithms (GAs), to simultaneously minimize the displacement of the building's top story and that of the base isolation system. In order to simultaneously minimize the objective functions, a fast and elitist non-dominated sorting genetic algorithm (NSGA-II) approach is used to find a set of Pareto-optimal solutions. The optimal values of the parameters of the base isolators, namely: their mass, stiffness, and damping ratio are evaluated using the GAs by taking into account the nonlinearity of the isolator bearings to minimize the objective functions. Moreover, in order to solve the undesirable horizontal displacement of the lead-rubber bearings, a new method called the "independent story" (IS) system is proposed in this investigation. This system works as a big tuned mass damper (TMD) system, without using any additional damping or stiffness devices except those of the structure itself. Either one full story of the building or even a part of one story can be considered the IS system. For a numerical example, a ten-story building located in Mashhad, Iran is chosen. From the numerical study, the NSGA-II approach was found to be strongly effective in evaluating the optimal values of the parameters of the isolator bearings and minimizing the structural responses.

1. Introduction

Mitigating the damage induced by dynamic loads, especially in seismic regions, is one of the most important interests in structural engineering. In traditional design methods, structure protection against earthquake loading was basically based on the energy dissipation through the inelastic deformation of structural elements. While, now this methodology is moving to use the structural control systems, such as passive and active control devices, to reduce the structural response and ensure minimal damage to the structural systems. In recent years, many studies have investigated different structural control systems [1–5]. Moreover, researchers

*Corresponding author. Tel.: +98 911 3310919; fax: +98 131 6690271.
E-mail address: pourzeynali@guilan.ac.ir (S. Pourzeynali).

0022-460X/$ - see front matter © 2007 Elsevier Ltd. All rights reserved.
doi:10.1016/j.jsv.2007.10.008

have performed significant studies on optimization algorithms in structural control devices [6–11]. However, despite this progress, challenges remain in better understanding these techniques to develop vibration control schemes.

Base isolation systems have been used on bridges since the early 1970s and on buildings from the late 1970s. The seismic base isolation technique is globally accepted and recognized as an effective technology to reduce the seismic effects on strategically important structures, such as hospitals, schools, bridges, and so on. The fundamental philosophy of base isolation systems is to reduce the response of the structures by providing a flexible layer between the foundation and base of the structure such that, ideally, the ground below the structure can move without transmitting these motions into the structure. The isolation system generally has low horizontal stiffness; therefore, it shifts the fundamental frequency of the structure to a value that is much lower than both its fixed-base frequency and the predominant frequency content of the earthquakes. Thereby, the amount of force that can be transferred to the structure is drastically reduced. The first dynamic mode of the isolated structure involves deformation only in the isolation system, the structure above being effectively rigid. The higher modes that produce deformation in the structure are orthogonal to the first mode, and consequently, to the ground motion. These higher modes do not participate in the motion, so that the high energy in the ground motion at these higher frequencies cannot be transmitted into the structure. The isolation system does not absorb the earthquake energy, but rather defects it through the dynamics of the system. This effect does not depend on damping, though a certain level of damping is beneficial to suppress possible resonance at the isolation frequency [12]. Flexibility and damping are provided in a single unity by laminated rubber bearing (LRB) systems. However, as a drawback, these have very little inherent damping and were not rigid enough to resist service loads, such as wind. In the early 1980s, developments in rubber technology lead to new rubber compounds termed high-damping rubbers (HDRs). These compounds produced bearings that had high stiffness at low shear strains, but a reduced stiffness at higher strain levels. Upon unloading, these bearings formed a hysteresis loop that had a significant amount of damping [13].

Since 1970, many research studies have investigated applications of elastomeric bearing isolators for structural seismic protection. The isolator systems developed therein have been utilized in a number of structures around the world, including nuclear facilities. Additionally, researchers in Europe, Japan, New Zealand, and the United States have developed their own types of base isolation systems, which have also been implemented in a variety of projects. However, despite the solid theoretical background of these systems, research efforts are still focusing on their application in structural vibration control.

In this paper, a multi-objective optimal genetic algorithm (MOGA) is used to design an isolation system for seismically excited high-rise building structures. The displacement response of the building's top story and that of the base isolators relative to the ground are selected as the two objectives for simultaneous minimization. For this purpose, a fast and elitist non-dominated sorting genetic algorithm (NSGA-II) approach [14] is used to find a set of Pareto-optimal solutions.

Moreover, in order to solve the undesirable horizontal displacement of the lead-rubber bearings, a new method called the "independent story" (IS) system is proposed in this investigation. In this new method, the independent story is considered to be between the $(i-1)$th and $(i+1)$th stories, without having any connection to the $(i+1)$th story. Either one full story of the building or even a part of one story can be considered the IS system. The combination of linear high-damping base-isolation systems with this IS system, significantly reduces the building's responses, simultaneously keeping the base displacement much lower than that achieved by the bilinear isolators.

2. Assumptions

The following simplified assumptions are made in the analyses [2,3]:

a. The main building is assumed to remain within the elastic limit during the earthquake excitation. Since the base isolation system reduces the building response to a relatively low value, this assumption is reasonable.
b. The building is modeled as a shear-type structure having one lateral degree of freedom at each story level (lumped mass and rigid floor assumption).

c. The columns providing the lateral stiffness are inextensible and weightless.
d. The system is subjected to a single horizontal component of the earthquake ground motion (single-support excitation assumption).
e. No soil–structure interaction is considered in the analyses.

3. Structural model of the base-isolated building

Fig. 1 shows the idealized mathematical model of the N-story, base-isolated, building structure considered in the present study.

For the system under consideration, the governing equations of motion are obtained by considering the equilibrium of forces at the location of each degree of freedom. For a fixed-base building (without any isolation system), these can be written as [12]

$$\mathbf{M}\ddot{\mathbf{U}} + \mathbf{C}\dot{\mathbf{U}} + \mathbf{K}\mathbf{U} = -\mathbf{M}\mathbf{R}\ddot{u}_g, \tag{1}$$

where $\mathbf{M}$, $\mathbf{C}$, and $\mathbf{K}$ are the structural mass, damping, and stiffness matrices, respectively, $\mathbf{U}$ is the relative displacement vector of the building with respect to the ground, $\mathbf{R}$ is the influence vector, $\ddot{u}_g$ is the earthquake ground acceleration, and a dot denotes the time derivative. For a seismically isolated structure with base mass m_b, the governing equation of motion for the building alone can be written as [12]

$$\mathbf{M}\ddot{\mathbf{V}} + \mathbf{C}\dot{\mathbf{V}} + \mathbf{K}\mathbf{V} = -\mathbf{M}\mathbf{R}(\ddot{u}_g + \ddot{v}_b), \tag{2}$$

where $\mathbf{V}$ is the displacement vector of the building stories relative to the base slab; and v_b is the relative displacement of the base slab with respect to the ground. Also, the overall equation of motion of the combined building and base slab can be written as [12]

$$\mathbf{R}^{\mathrm{T}}\mathbf{M}\ddot{\mathbf{V}} + \left(\sum_{i=1}^{n} m_i + m_b\right)\ddot{v}_b + c_b\dot{v}_b + k_b v_b = -\left(\sum_{i=1}^{n} m_i + m_b\right)\ddot{u}_g, \tag{3}$$

where n is the number of stories of the building; k_b and c_b are the stiffness and damping of the base isolator system, and m_i is the mass of the building's ith story.

By combining Eqs. (2) and (3), the general equation of motion for the combination of the seismically isolated building structure and the base slab can be expressed in matrix form as the following [12]:

$$\mathbf{M}^*\ddot{\mathbf{V}}^* + \mathbf{C}^*\dot{\mathbf{V}}^* + \mathbf{K}^*\mathbf{V}^* = -\mathbf{M}^*\mathbf{R}^*\ddot{u}_g \tag{4}$$

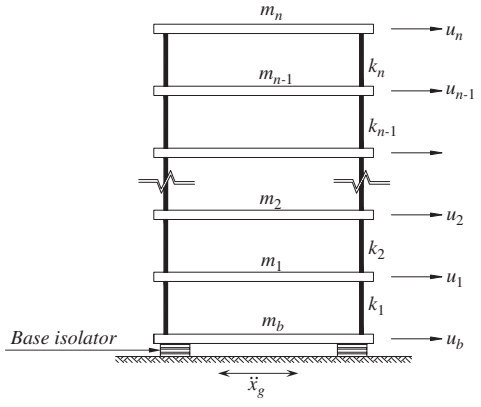

Fig. 1. Mathematical model of an N-story base-isolated building structure.

in which

$$\mathbf{M}^* = \begin{bmatrix} M & \mathbf{R}^T\mathbf{M} \\ \mathbf{MR} & \mathbf{M} \end{bmatrix}, \quad \mathbf{C}^* = \begin{bmatrix} c_b & \mathbf{0} \\ \mathbf{0} & \mathbf{C} \end{bmatrix}, \quad \mathbf{K}^* = \begin{bmatrix} k_b & \mathbf{0} \\ \mathbf{0} & \mathbf{K} \end{bmatrix}, \quad \mathbf{R}^* = \begin{bmatrix} 1 \\ \mathbf{0} \end{bmatrix}, \quad \mathbf{V}^* = \begin{bmatrix} v_b \\ \mathbf{V} \end{bmatrix},$$
$$M = m_b + \sum_{i=1}^{n} m_i, \tag{5}$$

where $\mathbf{0}$ is a zero matrix.

In order to solve Eq. (1), it is rewritten in state-space as

$$\dot{\mathbf{Z}} = \mathbf{A}_1\mathbf{Z} + \mathbf{B}_1\mathbf{P}, \tag{6}$$

where $\mathbf{Z}$ is the state vector, $\mathbf{A}_1$ the state matrix, and $\mathbf{B}_1$ is the input matrix. These are given as

$$\mathbf{Z} = \begin{Bmatrix} \mathbf{U} \\ \dot{\mathbf{U}} \end{Bmatrix}, \tag{7a}$$

$$\mathbf{A}_1 = \begin{bmatrix} \mathbf{0} & \mathbf{I} \\ -\mathbf{M}^{-1}\mathbf{K} & -\mathbf{M}^{-1}\mathbf{C} \end{bmatrix}, \quad \mathbf{B}_1 = \begin{bmatrix} \mathbf{0} \\ \mathbf{I} \end{bmatrix} \quad \text{and} \quad \mathbf{P} = -\mathbf{R}\ddot{u}_g(t), \tag{7b}$$

where $\mathbf{I}$ is an identity matrix.

The same procedure is used to solve Eq. (4).

4. Elastomeric base isolation systems

Most types of isolation systems provide damping that is classified as hysteretic damping, a function of displacement. Using known relationships, hysteretic damping can be converted to the equivalent viscous damping, damping which is a function of velocity. In most practical isolators, the hysteretic damping decreases with displacement after peaking at a relatively small displacement. Unfortunately, this trend is the opposite of what is sought for an ideal isolation system. A large earthquake produces a large displacement, where maximum damping is then required to control the displacement and force. These characteristics become most problematic when the design is for two level earthquakes, such as the design-basis earthquake (DBE) and maximum capable earthquake (MCE) levels defined by the uniform building code (UBC). At DBE levels of earthquake, damping of 15–20% can generally be achieved, while in a high seismic zone the damping at MCE load levels will often not exceed 10–12% [13].

When the travel path of the earthquake waves from the epicenter to the site is such that the earthquake motion at the site has a long period, this can cause resonance in the isolated structure. In this situation, the isolation systems may have a reverse effect and actually increase the response of the structure rather than reduce it. Examples of this phenomenon have been reported in Mexico City and Budapest. On the other hand, near-fault effects cause large velocity pulses close to the fault rupture location. Effects are greatest within 1 km of the rupture, but extend out to 10 km. The UBC provisions require that near-fault effects should be included by increasing the seismic loads by some factors. In time history dynamic analysis, this can be incorporated by including time histories reflecting near-fault effects. The near-fault record produces a much greater response than the more distance record. The isolation system is being used in near-fault locations, but the cost is usually higher and the evaluation more complex. In realistic design practice, any structure near a fault should be evaluated for the "fling" effect, which is characterized by a long period, high-velocity pulse in the ground acceleration record. This effect is not peculiar to the isolated structures [13].

The present investigation is a research study whose main objective is to use a multi-objective optimization solution to minimize simultaneously the seismically isolated building's top story displacement and that of the base isolation system. Therefore, the far- and near-fault effects are implicitly considered in the earthquake acceleration time history records selected for dynamic analysis of the building. Explicitly, then, minimal attention is given to this behavior of the base-isolated building, though it is critical in real design practice.

Generally, many different systems of isolators are proposed and patented each year. In this investigation, some elastomeric base isolation systems are studied. Their brief descriptions are provided in the following.

4.1. Laminated rubber bearings

The main components of the LRB systems are the rubber plates and steel shims built into a single unit. The internal reinforcing plates reduce the lateral bulging of the bearings and increase the vertical stiffness [12]. The dominant feature of the LRB systems is the parallel action of the linear spring and damping [2]. However, the LRB may exhibit hysteretic and stiffening behavior at large deformations. The restoring force developed in the bearing, F_b, is given by [2]

$$F_b = c_b\dot{v}_b + k_b v_b, \tag{8}$$

where c_b and k_b are, respectively, the damping and stiffness of LRB systems. The value of F_b given in Eq. (8) is used in Eq. (3). The stiffness and damping of LRB systems are selected to provide the specific values of two parameters, the isolation time-period (T_b) and the damping ratio (ξ_b), defined as [2]

$$T_b = 2\pi\sqrt{\frac{M}{k_b}}, \tag{9}$$

$$\xi_b = \frac{c_b}{2M\omega_b}, \tag{10}$$

where M is defined in Eq. (5), and $\omega_b = 2\pi/T_b$ is the isolation frequency.

4.2. Lead-rubber bearings

Lead-rubber bearings were invented in New Zealand in 1975 and have been used extensively in New Zealand, Japan, and the United States [12]. These systems are generally referred as N–Z systems. N–Z bearings are similar to LRB systems, but in order to provide an additional means of energy dissipation and initial rigidity against minor earthquakes and winds, a central lead-core system is used [15,16]. The force-deformation behavior of the N–Z bearings is generally represented by nonlinear characteristics (Fig. 2). In the present study, the bilinear hysteretic model of these isolators is used [3]. The bilinear hysteretic loop, as shown in Fig. 2, is characterized by three parameters: (1) yield strength F_y, (2) elastic and plastic stiffness values k_{b1} and k_{b2}, respectively, and (3) yield displacement v_y [3]. The restoring force developed in these isolation bearings can also be represented by Eq. (8), by replacing the k_b with appropriate k_{b1} and k_{b2} in the elastic and

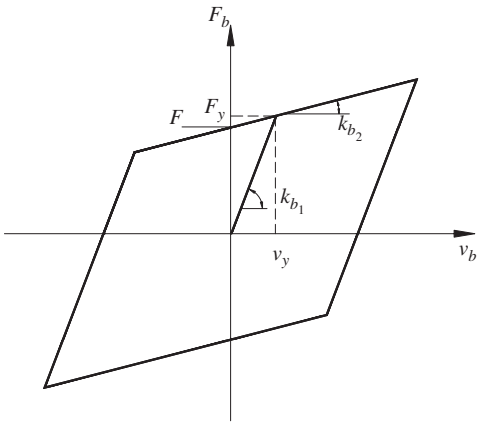

Fig. 2. Bilinear hysteretic model of the lead-rubber bearings used in this study.

plastic phases, respectively. In this study, the values of v_y and $\gamma = k_{b2}/k_{b1}$ are taken to be about 2.50 cm and 0.142, respectively [3,17].

5. Genetic algorithms

In civil engineering design, especially in designing complex structures, optimization has a special importance and value. Basically, the optimization process finds a set of quantities for the design parameters that yield optimal values of the objective functions. Most optimization methods used in the design of structural vibration control systems are traditional, gradient-based search techniques. However, for these techniques, there are difficulties, both in selecting a suitable continuously differentiable cost function, as well as in incorporating the nonlinearities involved in the problem. Compared to these gradient-based methods, genetic algorithms (GAs) are very simple and powerful optimal search techniques, because GAs do not need a continuous and differentiable function to solve the problem, and are able to take into account the nonlinearities (if any) of the problem.

GAs have been applied as effective optimization search techniques in civil engineering structural vibration control design. GAs are stochastic search techniques based on the mechanism of natural selection and natural genetics. GAs start with an initial set of random selections, called a population. Each individual in the population is called a chromosome, representing a solution to the problem at hand. The chromosomes evolve through successive iterations, called generations. During each generation, the chromosomes are evaluated using some measures of fitness.

In GAs, three main operators are used: selection, crossover, and mutation. Usually, initialization is assumed to be random. Recombination typically involves crossover and mutation to yield offspring. In fact, there are only two kinds of operations in GAs: (1) genetic operation, i.e., crossover or mutation, and (2) evolution operation, i.e., selection. Crossover is the main genetic operator. The performance of GAs depends, to a great extent, on the performance of the crossover operator used [18].

In every generation, strings are selected into the mating pool based on their relative fitness. The fitter strings are given a better chance of passing their genes into the next generation [19]. In most practices, a roulette wheel approach is adopted as the selection procedure. This is a fitness-proportional selection and can select a new population with respect to the probability distribution based on fitness values. Then, a wheel is constructed according to these probabilities. The selection process relies on spinning the roulette wheel population-size times; each time a single chromosome is selected for the new population. This is termed stochastic sampling [18].

The crossover used here is a one-cut-point method, which randomly selects cut-point and exchanges the right parts of parents to generate offspring. The probability of crossover is set as $P_c = 0.25$; thus, on average, 25% of chromosomes undergo crossover.

Mutation alters one or more genes with a probability equal to the mutation rate. The probability of mutation is set as $P_m = 0.01$; thus, on average, 1% of the total bits of the population undergoes mutation.

5.1. Multi-objective optimization

In many realistic problems, several goals must be simultaneously satisfied to obtain an optimal solution. However, sometimes these multiple objectives, which must be simultaneously satisfied, conflict [20]. The multi-objective optimization method is the common approach to solve this type of problem. Multi-objective optimization, in general, can be defined as [21]

Find the vector $\mathbf{X}^* = \left[x_1^*, x_2^*, \ldots, x_n^*\right]^{\mathrm{T}}$ which will satisfy the m inequality constraints:

$$g_i(\mathbf{X}) \geqslant 0, \quad i = 1, 2, \ldots, m \tag{11}$$

and the p equality constraints:

$$h_i(\mathbf{X}) = 0, \quad i = 1, 2, \ldots, p \tag{12}$$

and will optimize the vector function:

$$\mathbf{F}(\mathbf{X}) = \left[f_1(x), f_2(x), \ldots, f_n(x)\right]^{\mathrm{T}}, \tag{13}$$

where $\mathbf{X} = [x_1, x_2, \ldots, x_n]^T$ is the vector of decision variables. In other words, from all the sets of all numbers, determine which particular set $x_1^*, x_2^*, \ldots, x_n^*$ satisfying Eqs. (11) and (12) yields the optimal values of all the objective functions [20]. The vector $\mathbf{X}^* = \left[x_1^*, x_2^*, \ldots, x_n^*\right]^T$ is denoted the optimal solution that can be obtained based on the Pareto-optimality definition given here.

A point $\mathbf{X}^* \in \mathbf{F}$ is Pareto-optimal (minimum) if, for every $\mathbf{X} \in \mathbf{F}$ and $\mathbf{I} = \{1, 2, \ldots, n\}$, either

$$\forall i \in \mathbf{I} : f_i(\mathbf{X}) = f_i(\mathbf{X}^*) \tag{14}$$

or there is at least one $i \in \mathbf{I}$ such that

$$f_i(\mathbf{X}) \succ f_i(\mathbf{X}^*), \tag{15}$$

where $\mathbf{F}$ is the feasible region of the search space. In words, this definition indicates that $\mathbf{X}^*$ is Pareto-optimal if there exists no feasible vector $\mathbf{X}$ which would decrease some criterion without causing a simultaneous increase in at least one other criterion [21]. In a Pareto-optimal search method, a vector $\mathbf{U} = \{u_1, u_2, \ldots, u_n\}^T$ is said to dominate the vector $\mathbf{V} = \{v_1, v_2, \ldots, v_n\}^T$ (denoted by $\mathbf{U} \preccurlyeq \mathbf{V}$) if and only if $\mathbf{U}$ is less than $\mathbf{V}$, i.e. $\forall i \in \{1, 2, \ldots, n\}, u_i \preccurlyeq v_i \wedge \exists i \in \{1, 2, \ldots, n\} : u_i \prec v_i$ [21].

In this research study, to find the Pareto-optimal solutions, the fast and elitist NSGA-II approach proposed by Deb et al. in 2002 [14] is used. In this approach, to sort a population of size N according to the level of non-domination, each solution must be compared with every other solution in the population to determine if it is dominated. At this stage, all individuals in the first non-dominated front are found. In order to find individuals of the next front, the solutions of the first front are temporarily discounted, and the above procedure is performed again. The procedure is repeated to find subsequent fronts [14]. For details about the NSGA-II approach, refer to Ref. [14].

In optimization studies that include multi-objective optimization problems, the main objective is to find the global Pareto-optimal solutions, representing the best possible objective values. However, in practice, users may not always be interested in finding the global best solutions, particularly if these solutions are very sensitive to variable perturbations. In such cases, practitioners are interested in finding robust solutions that are less sensitive to small changes in variables [22]. In past decades, many studies have been performed on finding robust solutions to single-objective [23,24] and multi-objective optimization problems [22]. In the present study, the central focus is to find the global Pareto-optimal solutions; the sensitivity of such solutions to small changes in the variables, or the robustness of the solutions, is not studied.

In the present study, horizontal displacement of the building's top story and that of the base isolation system are considered the objective functions to be simultaneously minimized. Furthermore, the mass, stiffness, and damping ratios of the base isolators are the decision variables to be evaluated through the multi-objective optimization process.

6. Earthquake ground-motion time histories

For time history dynamic analysis of the structures, the earthquake inputs must be specified in terms of free-field strong ground-motion accelerograms. For this purpose, correction processing is performed on the uncorrected accelerograms, including a band-pass filtering of low- and high-frequency noises, an instrument correction, and a base-line correction. All corrected accelerograms are scaled individually so that they are representative of accelerograms compatible with a design response spectrum. The time histories selected from sites within 15 km of major active faults should incorporate near-fault phenomena. In the present study, 18 worldwide strong ground-motion accelerograms are selected, corrected and scaled as needed, and used in the analyses. Further explanations about these accelerograms are provided in the next section.

7. Numerical analysis

For numerical evaluation of the isolation systems and effectiveness of GA optimizers proposed in this investigation, a realistic ten-story building, located in Mashhad, Iran, is selected. For this building, the mass

and stiffness matrices are calculated using the matrix analysis procedure. The damping matrix of the building is also assumed to be proportional to the mass and stiffness matrices (Rayleigh method). To calculate the proportionality coefficients, modal damping ratios of the first two modes were assumed to be about 2% of the critical value. The building is a steel structure with braced frame systems. Analysis was performed for a 2-D, 7-bayes planar-braced ten-story frame of the building. For this typical planar frame of the building, the stiffness and mass matrices are provided in Eqs. (16) and (17).

$$\mathbf{K} = \begin{bmatrix} 2.3788 & -1.2161 & 0 & 0 & 0 & 0 & 0 & 0 & 0 & 0 \\ -1.2161 & 2.3371 & -1.1210 & 0 & 0 & 0 & 0 & 0 & 0 & 0 \\ 0 & -1.1210 & 2.2094 & -1.0883 & 0 & 0 & 0 & 0 & 0 & 0 \\ 0 & 0 & -1.0883 & 2.1767 & -1.0883 & 0 & 0 & 0 & 0 & 0 \\ 0 & 0 & 0 & -1.0883 & 2.0159 & -0.9276 & 0 & 0 & 0 & 0 \\ 0 & 0 & 0 & 0 & -0.9276 & 1.7917 & -0.8641 & 0 & 0 & 0 \\ 0 & 0 & 0 & 0 & 0 & -0.8641 & 1.6509 & -0.7868 & 0 & 0 \\ 0 & 0 & 0 & 0 & 0 & 0 & -0.7868 & 1.4486 & -0.6617 & 0 \\ 0 & 0 & 0 & 0 & 0 & 0 & 0 & -0.6617 & 1.3235 & -0.6617 \\ 0 & 0 & 0 & 0 & 0 & 0 & 0 & 0 & -0.6617 & 0.6617 \end{bmatrix} 1e9(\mathrm{N\,m^{-1}}) \tag{16}$$

and

$$\mathbf{M} = \mathrm{diag}(3.812, 3.79, 3.806, 2.743, 2.803, 2.783, 2.763, 2.763, 2.753, 2.745)1e5\,\mathrm{kg}. \tag{17}$$

Moreover, it should be noted that all ten vibrational modes of the building are considered in the analysis, and the first 5 modal frequencies are given as: 1.46, 3.86, 6.27, 8.69, and 10.84 Hz.

The building was analyzed for an ensemble of 18 worldwide earthquake acceleration records about which, for some of the most important earthquakes, the relevant details are given in Table 1. As seen from the table, some of these accelerograms may incorporate the near-fault effect in the analyses.

First, a seismic base isolation system for the example building is analyzed for the above-mentioned earthquakes. The results are compared with those of a fixed-base building. In this step, the structural parameters of the base isolation system are taken from Refs. [2,3] as the initial values:

$$m_0 = m_b/m_1 = 1.0, \quad k_0 = k_b/k_1 = 0.10, \quad \xi_b = c_b/(2M\omega_b) = 0.10, \quad \omega_b = \sqrt{k_b/M},$$

Table 1
The most important earthquake accelerograms considered in this study

Earthquake	Country	Station	Year	Magnitude (M_W)	Component	PGA (g)	Hypocentral dist. (km)	Closest dist. to fault (km)
Kobe	Japan	Takatori	1995 (January)	6.9	EW	0.615	22.2	1.5
Loma Prieta	US (California)	Watsoville	1989 (October)	7.0	EW	0.601	25.4	11.8
Northridge	US (California)	Tarzana	1994 (January)	6.7	EW	0.990	19.8	16.7
El Centro	US (California)	Imperial valley (Array Sta. 9)	1940 (May)	6.9	NS	0.348	12.2	–
Bam	IR Iran	Bam	2003 (December)	6.5	NS	0.793	10.2	–
Sarein	IR Iran	Kariq	1997 (February)	6.1	EW	0.615	60.1	–
Zanjiran	IR Iran	Zanjiran	1994 (June)	6.1	NS	1.09	12.2	–

where ξ_b is the damping ratio of base isolation system, m_1 and k_1 are the mass and stiffness of the building first story, m_0 and k_0 are the mass and stiffness ratio of the base isolation system, ω_b is the natural circular frequency of the base isolation system, and M is given in Eq. (5).

By considering the above values and using MATLAB software, equations of motion of the building are solved and the results are shown in Table 2 for the fixed-base, and in Table 3 for the base-isolated building supported on isolators with linear behavior. It should be mentioned that, for brevity, the tables only include the results of the four most important earthquakes (Kobe, El Centro, Loma Prieta, and Northridge Earthquakes, mentioned in Table 1), as well as the ensemble average values of the responses for the 18 reference earthquakes.

As seen from the tables, displacements of the isolated building are significantly reduced. In this case, an average reduction of 43.74% is obtained in the building's top story horizontal displacement response. For comparison, time histories of the building's top story displacement and acceleration responses for both fixed-base and isolated buildings are shown in Fig. 3a and b, respectively. Here also, the same suppression effectiveness can be seen. The problem associated with this type of vibrational response protection system is that the base displacement is still relatively high in comparison with that of the building stories.

Now, using a GA optimizer, parameters of the isolators, including their stiffness, damping, and the base mass, are calculated to minimize simultaneously both the building's top story and base isolator displacements using the multi-objective optimization procedure given in the following section. For this purpose, the variation domains (domain constraints) of these parameters are assumed to be

$$D_{m_0} = [0.10, 1.50], \quad D_{\xi_b} = [0.02, 0.30], \quad D_{k_0} = [0.02, 0.20],$$

where D_{m0}, $D_{\xi b}$ and D_{k0} are, respectively, the domains of mass, damping, and stiffness ratios of the base isolators.

Table 2
Stories' displacements (m) in the fixed-base building

Earthquakes	Stories of the building									
	1st	2nd	3rd	4th	5th	6th	7th	8th	9th	10th
Kobe	0.049	0.094	0.141	0.186	0.227	0.269	0.307	0.339	0.365	0.378
El Centro	0.020	0.038	0.057	0.073	0.088	0.104	0.120	0.134	0.145	0.151
Loma Prieta	0.035	0.067	0.098	0.171	0.153	0.179	0.202	0.222	0.237	0.245
Northridge	0.025	0.049	0.075	0.101	0.126	0.152	0.178	0.201	0.220	0.230
Ensemble average responses (m)	0.0302	0.0578	0.0856	0.1304	0.1340	0.1573	0.1791	0.1996	0.2004	0.2245

Table 3
Horizontal displacements (m) in the isolated building supported on elastomeric bearings with linear behavior

Earthquakes	Stories of the building										
	Base	1st	2nd	3rd	4th	5th	6th	7th	8th	9th	10th
Kobe	0.173	0.034	0.064	0.093	0.120	0.144	0.168	0.189	0.208	0.223	0.230
El Centro	0.094	0.018	0.033	0.048	0.060	0.072	0.084	0.094	0.103	0.111	0.114
Loma Prieta	0.139	0.026	0.049	0.071	0.090	0.108	0.126	0.141	0.154	0.165	0.170
Northridge	0.132	0.024	0.042	0.058	0.070	0.082	0.098	0.113	0.127	0.139	0.145
Ensemble average responses (m)	0.099	0.019	0.036	0.052	0.066	0.078	0.092	0.104	0.114	0.122	0.126
Ensemble average reduction ratios (%)	–	36.94	38.45	39.88	49.6	41.35	41.61	42.08	42.95	39.06	43.74

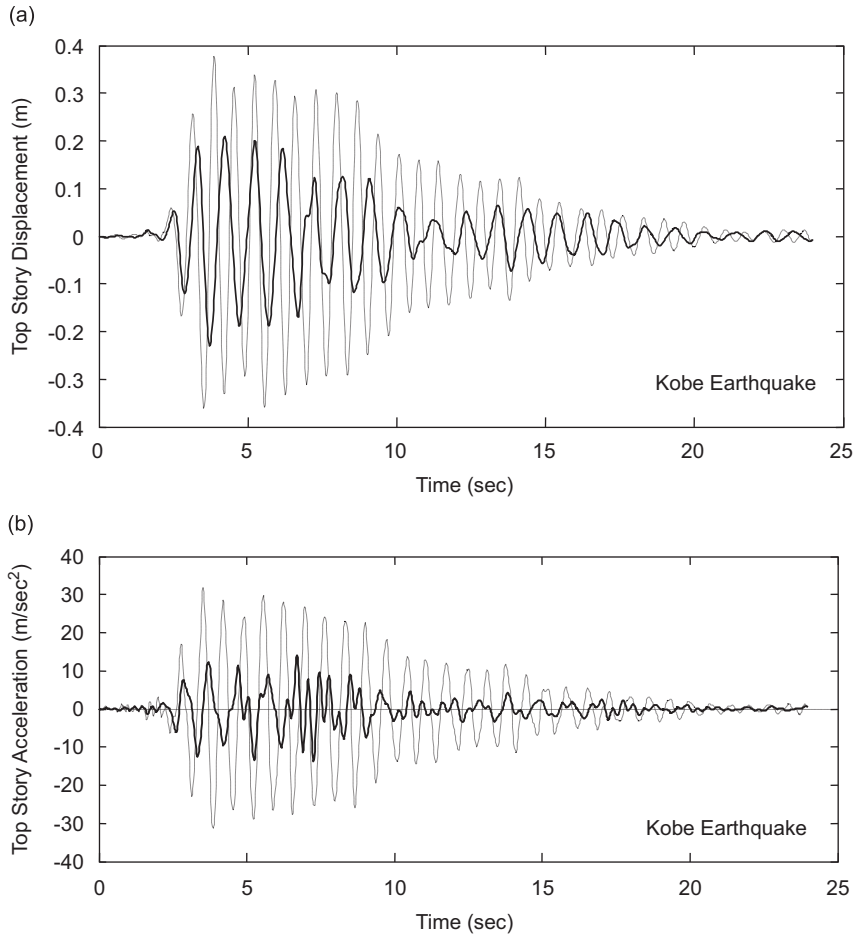

Fig. 3. Comparison of the fixed-base and isolated building's top story responses: (a) displacement and (b) acceleration (------ non-isolated, and —— isolated).

7.1. Multi-objective optimization

In this section, in order to minimize simultaneously both the building's top story displacement and that of the base isolation system, a multi-objective GA optimizer is used. For this purpose, each objective function is separately minimized by first using a single-objective GA optimizer. Then, a fast and elitist NSGA-II approach is used to find Pareto-optimal solutions in Pareto space.

As the GA is a stochastic search methodology, it is difficult to specify formal convergence criteria. The common practice is to terminate the GA after a predefined number of generations, and then test the quality of the solutions. If the solutions are unacceptable, then the GA may be restarted for more generation numbers or by taking fresh initial values. The multi-objective problem is solved utilizing a computer program developed in MATLAB software. For the single-objective GA optimizer, the following parameters are chosen [18]:

$$\text{Number of chromosomes} = 25, \quad \text{Number of generations} = 300,$$
$$\text{Probability of crossover, } P_c = 0.25 \quad \text{and} \quad \text{Probability of mutation, } P_m = 0.01.$$

The GA iterations terminated after 300 generations, and the best results for the parameters of base isolators are obtained as the following:

$$m_0 = 1.20, \quad k_0 = 0.05, \quad \xi_b = 0.25.$$

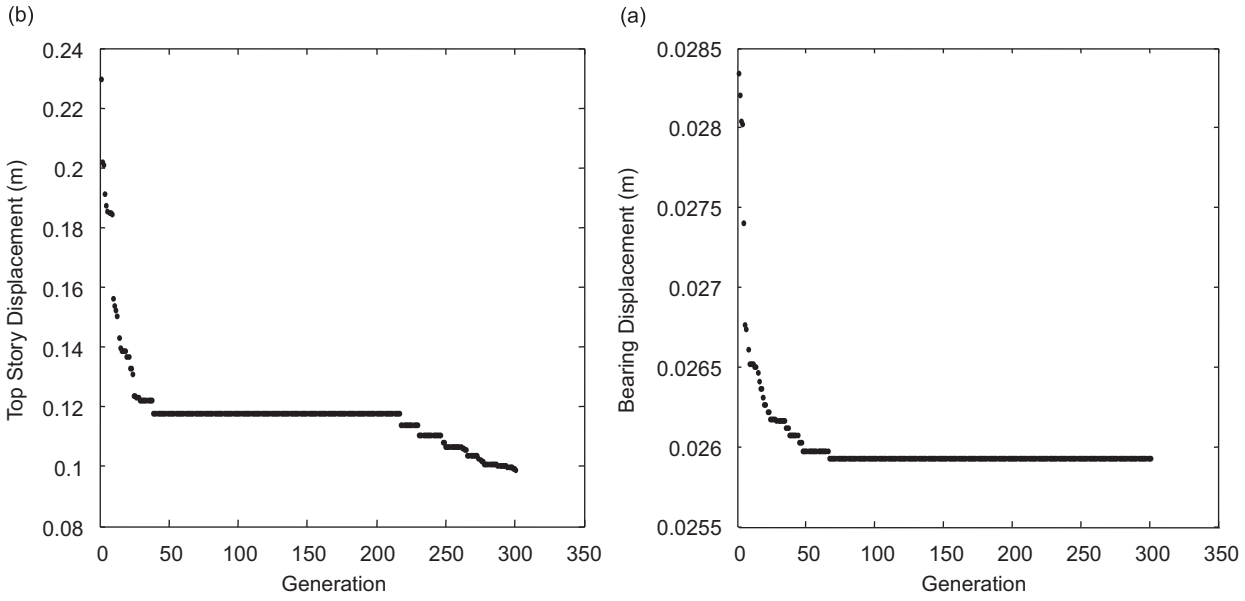

Fig. 4. Performance of genetic algorithm with single-objective function: (a) maximum displacement of seismic isolator with linear behavior and (b) maximum displacement of the isolated building's top story.

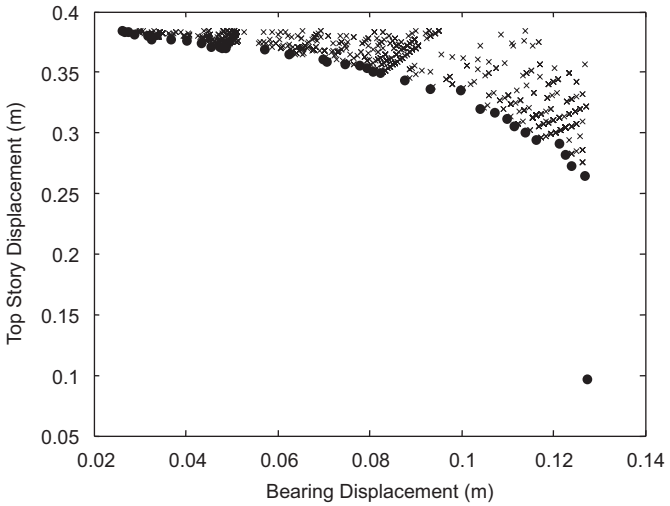

Fig. 5. Optimal points of the Pareto front and design range for base isolators with linear behavior (× feasible range, and ● Pareto front).

The results are shown in Figs. 4 and 5. Fig. 4 shows the results for each of the objective functions (top story and base isolator displacements) separately, and Fig. 5 shows the Pareto-optimal front diagram for the multi-objective problem. Moreover, the isolated building responses for four selected earthquakes, as well the ensemble average values of its stories' GA-optimized responses for the 18 reference earthquakes, are shown in Table 4. In the last row of the table, the reduction ratios on the building's story displacements are also shown. The table shows that NSGA-II is very effective at minimizing the objective functions and calculating the design parameters. On average, a reduction of 64.47% is obtained for the building's top story horizontal displacement response.

Table 4
Controlled responses (optimized by GA) of the isolated building supported on linear isolators

Earthquakes	Stories of the building										
	Base	1st	2nd	3rd	4th	5th	6th	7th	8th	9th	10th
Kobe	0.303	0.051	0.075	0.088	0.094	0.099	0.104	0.110	0.113	0.116	0.118
El Centro	0.168	0.025	0.044	0.056	0.063	0.068	0.073	0.082	0.090	0.095	0.097
Loma Prieta	0.207	0.032	0.053	0.065	0.070	0.074	0.084	0.094	0.100	0.104	0.107
Northridge	0.475	0.064	0.098	0.117	0.131	0.144	0.154	0.167	0.174	0.178	0.183
Ensemble average responses (m) (optimized by GA)	0.115	0.025	0.022	0.032	0.081	0.050	0.058	0.066	0.072	0.077	0.080
Ensemble average reduction ratios (%)	–	53.10	61.80	62.36	59.20	62.80	63.00	63.34	63.95	61.50	64.47

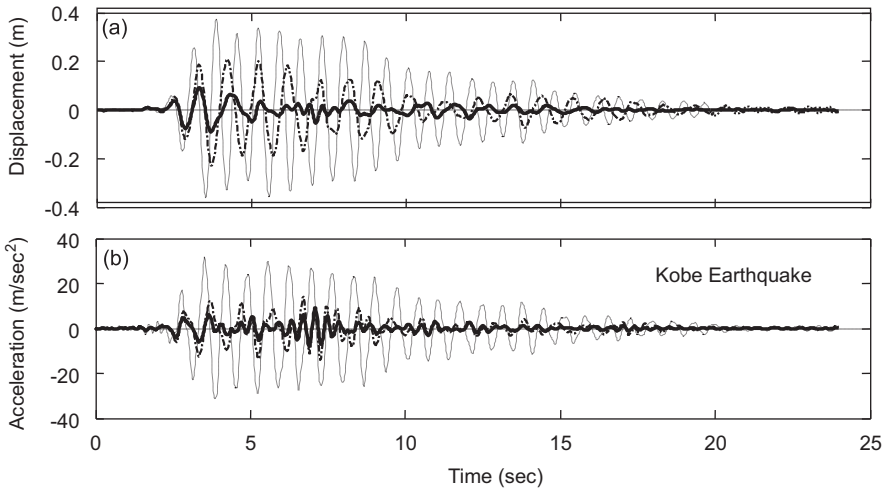

Fig. 6. Comparison of the controlled and uncontrolled responses of the building's top story for the Kobe earthquake: (a) displacement and (b) acceleration (——— non-isolated, -·-·-·- isolated, and ▬▬ optimized by GA).

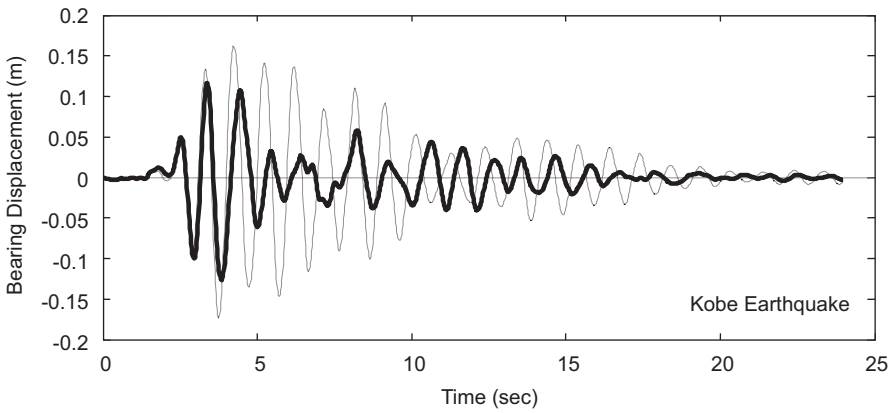

Fig. 7. Comparison of base isolator displacements with that optimized by GA (——— isolated, and ▬▬ optimized By GA).

Moreover, Figs. 6 and 7 compare the time histories of the controlled and uncontrolled responses of the building's top story and that of the base isolation system for the Kobe earthquake. The figures also show that NSGA-II is a very powerful tool to estimate parameters of the base isolators in order to reduce both the building and base isolator displacements.

7.2. Multi-objective optimization by considering nonlinear behavior of the bearings

Herein, the material nonlinearity of the isolator bearings has been taken into account by assuming that lead-rubber bearings have been used. For simplification, the nonlinear hysteretic curve of the bearings, as shown in Fig. 2, is divided into two linear parts (bilinear models).

The main parameters of the bilinear isolators are: the base mass, m_b (similar to the linear case); isolator stiffness in the elastic phase, k_{b1}, and its stiffness in the plastic phase, k_{b2}; its time period in the elastic phase and after yielding, T_{b1} and T_{b2}, respectively, which can be calculated by Eq. (18); and the yield displacement, v_y, which can be calculated for different isolators by experiments. Also, the ratio of k_{b2}/k_{b1}, defined as γ, can be obtained from experiments.

In this study, the values of v_y and γ are assumed to be about 2.5 cm and 0.142, respectively, as given in Refs. [3,17]. Finally, the damping ratio of the elastic phase, ξ_{b1}, and that of the plastic phase, ξ_{b2}, are defined by Eq. (19):

$$T_{b_1} = 2\pi\sqrt{(M/k_{b_1})}, \quad T_{b_2} = 2\pi\sqrt{(M/k_{b_2})}, \tag{18}$$

$$\xi_{b_1} = c_b T_{b_1}/(4\pi M), \quad \xi_{b_2} = c_b T_{b_2}/(4\pi M). \tag{19}$$

Here also, the same parameters of the linear isolators have been chosen for GA optimization:

$$\text{Number of initial populations} = 25, \quad \text{Number of generations} = 300,$$
$$P_c = 0.25, \quad \text{and} \quad P_m = 0.01.$$

In order to apply the multi-objective GA optimizer, each individual objective function was first optimized using a single-objective GA. The results are shown in Fig. 8a and b for displacement

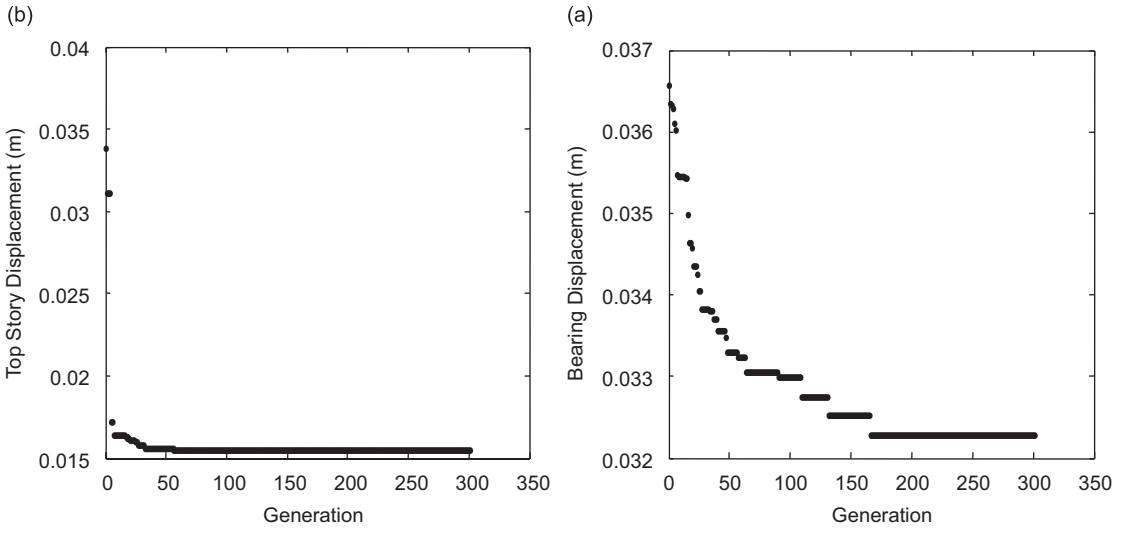

Fig. 8. Performance of the genetic algorithm with single-objective function: (a) maximum displacement of bilinear base isolator and (b) maximum displacement of the isolated building's top story.

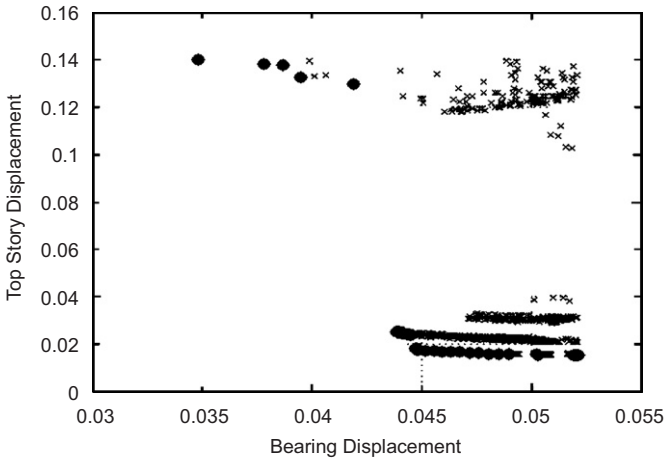

Fig. 9. Optimal points of the Pareto front and design range for bilinear isolators (× feasible range, and ● Pareto front).

Table 5
Horizontal displacements (m) of the isolated building after considering the nonlinearity of the bearings and optimization by GA

Earthquakes	Stories of the building										
	Base	1st	2nd	3rd	4th	5th	6th	7th	8th	9th	10th
Kobe	0.151	0.010	0.015	0.022	0.028	0.033	0.038	0.043	0.047	0.052	0.056
El Centro	0.289	0.025	0.040	0.054	0.061	0.064	0.067	0.070	0.071	0.073	0.074
Loma prieta	0.201	0.041	0.063	0.072	0.079	0.084	0.087	0.089	0.091	0.093	0.096
Northridge	0.271	0.024	0.038	0.051	0.058	0.062	0.065	0.067	0.068	0.068	0.068
Ensemble average responses (m) (optimized by GA)	0.218	0.018	0.029	0.037	0.044	0.049	0.052	0.056	0.059	0.062	0.064
Ensemble average reduction ratios (%)	–	34.71	49.50	56.45	66.44	63.84	67.05	68.71	70.46	69.34	71.68

of the building's top story and that of the base isolators. Then, using these results, the Pareto-optimal front diagram was obtained (Fig. 9), from which the following optimal values for bilinear isolators were extracted:

$$k_0 = k_{b_1}/k_1 = 0.40, \quad m_0 = m_b/m_1 = 0.35, \quad \xi_{b_1} = 0.19, \quad \xi_{b_2} = 0.50.$$

Table 5 shows the controlled responses of the building's stories for four selected earthquakes, the ensemble average responses for 18 reference earthquakes, and the ensemble average reduction ratios for the same reference earthquakes calculated for all stories of the building. From the table, the bilinear base isolators are shown to provide greater reduction in building response in comparison to the linear ones. An average reduction of 71.68% is obtained on the building's top story horizontal displacement response. Furthermore, Figs. 10 and 11 show effects of the linear and bilinear behavior of base isolators on the horizontal displacement of the building's top story and that of the base isolators. Fig. 11 shows that, due to plastic deformation of the bearings in bilinear isolators, the base displacement is greater than that of the linear case. This is the main drawback of these systems. Furthermore, Fig. 12 shows the hysteresis relationship between the bearing's horizontal deformation and the forces exerted through the building columns to the bearings. The figure shows that the maximum force exerted

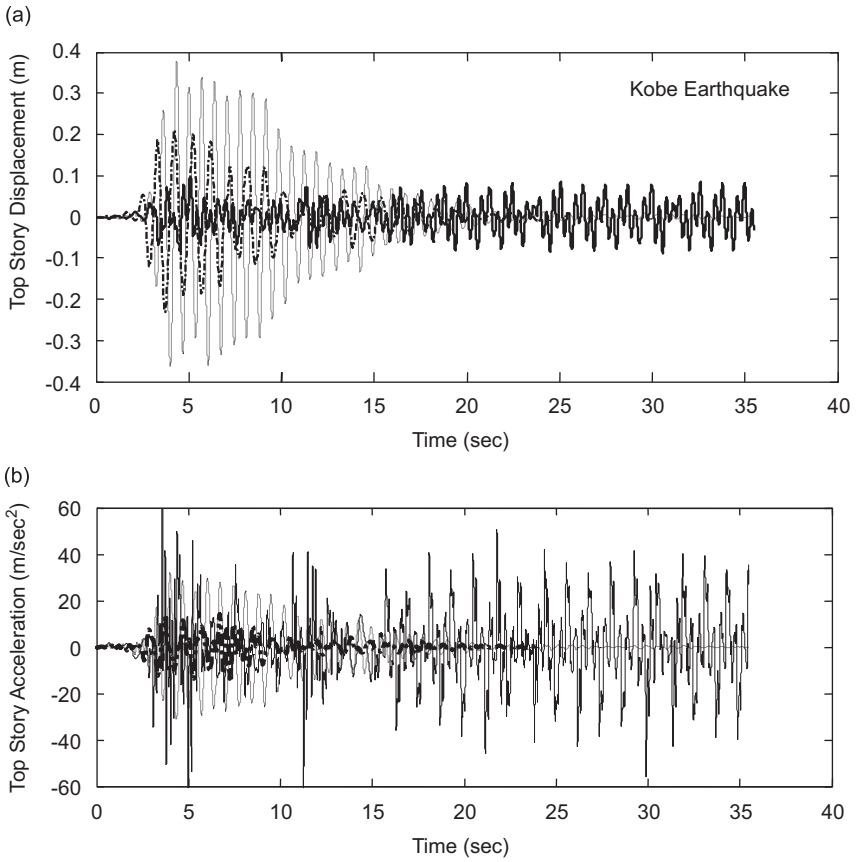

Fig. 10. Comparison of the controlled and uncontrolled responses of the isolated building's top story for linear and bilinear isolators optimized by GA: (a) horizontal displacement and (b) acceleration (—— non-isolated, ——— bilinear &GA, and -·-·-·- linear &GA).

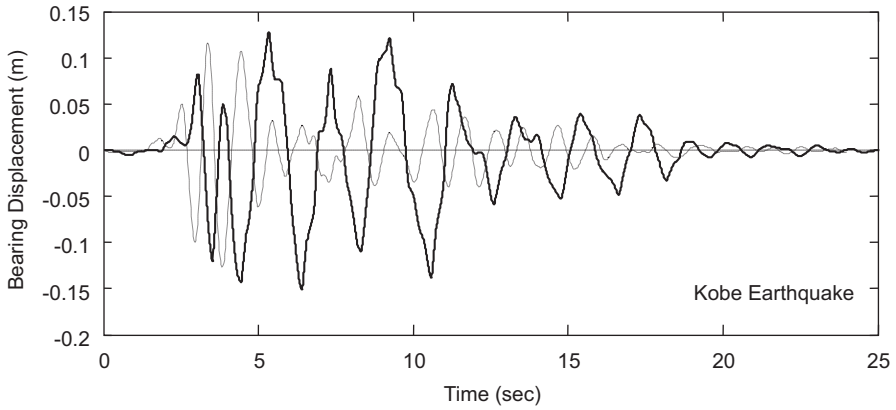

Fig. 11. Comparison of the linear and bilinear isolator displacements optimized by GA (——— bilinear &GA, and —— linear& GA).

on the bearings is about 3.2×10^6 N, which is a reasonable value based on the total columns of the building.

From this discussion, the horizontal displacement of the bilinear lead-rubber bearings is seen to be relatively high, and use of these systems, practically, may sometimes be problematic. Therefore, to overcome this deficiency, a new method called the "IS" system is proposed in this investigation. The combination of linear

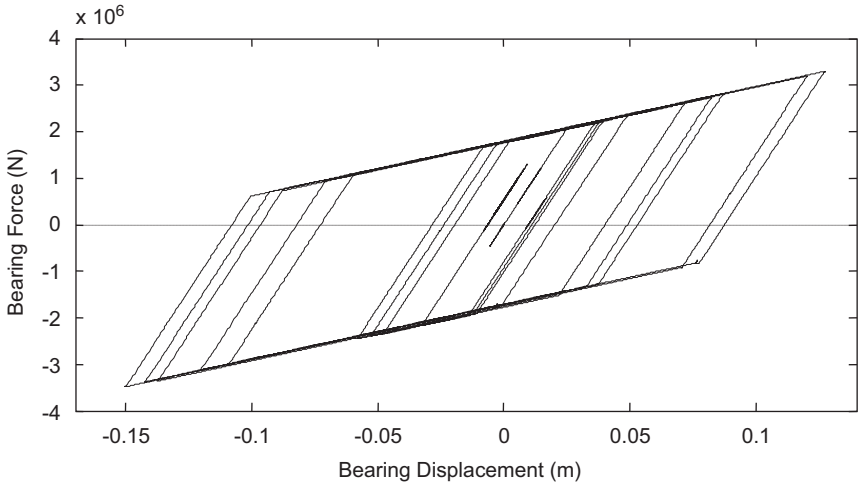

Fig. 12. Force–displacement diagram of the bilinear isolators (parameters optimized by GA).

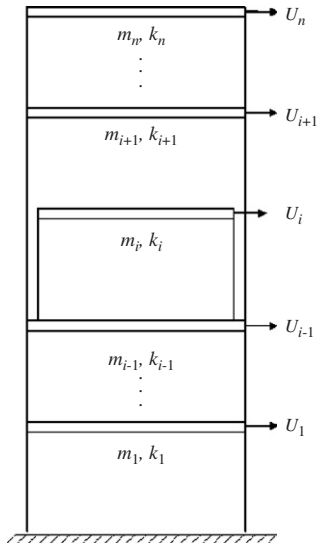

Fig. 13. Independent-story system, proposed in this investigation.

high-damping base-isolation systems with this "IS" system, as discussed in subsequent sections, would reduce the building's responses even more than the bilinear lead-rubber systems, simultaneously keeping the base displacement much lower than that achieved by the bilinear isolators.

7.3. "Independent story" system

As discussed above, in order to solve the undesirable horizontal displacement of the lead-rubber bearings, the IS system is proposed as a new method. In this new method, as shown in Fig. 13, the independent story is considered to be between the $(i-1)$th and $(i+1)$th stories, without having any connection to the $(i+1)$th story. In fact, the independent story system works as a big tuned mass damper (TMD) system, without using any additional damping or stiffness devices except those of the structure itself. It should be noted that either one full story of the building or even a part of one story can be considered as the independent story in this system.

The mass and stiffness matrices of the building, when the ith story is considered to be the IS system, can be developed as

$$\mathbf{M} = \mathrm{diag}(m_1, m_2, \ldots, m_{i-1}, m_{is}, m_{i+1}, \ldots, m_n) \tag{20}$$

and

$$\mathbf{K} = \begin{bmatrix} k_1+k_2 & -k_2 & 0 & & & & & & & & \\ -k_2 & & \cdot & & & & & & & & \\ & & & \cdot & & & & & & & \\ & & & & \cdot & & & & & & \\ & & 0 & -k_{i-1} & k_{i-1}+k_{\mathrm{is}}+k_{i+1} & -k_{\mathrm{is}} & -k_{i+1} & 0 & & & \\ & & & 0 & -k_{\mathrm{is}} & k_{\mathrm{is}} & 0 & 0 & & & \\ & & & & -k_{i+1} & 0 & k_{i+1}+k_{i+2} & -k_{i+2} & & & \\ & & & & & & & \cdot & & & \\ & & & & & & & & \cdot & & \\ & & & & & & & & & \cdot & -k_n \\ & & & & & & & & 0 & -k_n & k_n \end{bmatrix}, \tag{21}$$

where m_i and k_i are the mass and stiffness of the ith story, respectively, and m_{is} and k_{is} are the mass and stiffness of the independent story, respectively. Mass and stiffness of the independent story are taken proportional to its underlying story. In this study, the 6th story is considered to be the independent story; therefore, the proportionality coefficients for its mass and stiffness (m_{d0} and k_{d0}) are defined as

$$m_{d0} = \frac{m_{\mathrm{is}}}{m_5}, \quad k_{d0} = \frac{k_{\mathrm{is}}}{k_5}. \tag{22}$$

Table 6
Effectiveness of the proposed IS system in reducing the example building's responses

Building responses	Stories of the building										
	1st	2nd	3rd	4th	5th	6th	7th	8th	9th	10th	11th
Fixed base responses (m)	0.030	0.058	0.086	0.130	0.134	–	0.157	0.179	0.200	0.200	0.225
Ensemble average responses (m) (controlled by IS sys.)	.0144	.0274	0.040	0.052	0.063	0.064	0.072	0.083	0.092	0.100	0.104
Ensemble average reduction ratios (%)	52.17	52.61	52.99	60.02	53.18	–	54.41	53.91	53.87	50.05	53.51

Table 7
Effectiveness of the proposed IS-BS-GA system in reducing the example building's responses

Building responses	Stories of the building											
	Base	1st	2nd	3rd	4th	5th	6th	7th	8th	9th	10th	11th
Fixed base responses (m)	–	0.030	0.058	0.086	0.130	0.134	–	0.157	0.179	0.200	0.200	0.225
Ensemble average responses (m) (controlled by IS system)	0.158	0.007	0.028	0.018	0.023	0.027	0.028	0.030	0.033	0.037	0.039	0.040
Ensemble average reduction ratios (%)	–	77.7	52.5	79.2	82.8	80.1	–	81.2	81.4	81.7	80.5	82.1

At this point, to start investigating the effectiveness of the IS system in reducing the response of the example building, the initial values for m_{d0} and k_{d0} are chosen as

$$m_{d0} = 0.90 \text{ and } k_{d0} = 0.90$$

and the results of the building responses with this IS system (without any base isolation system) are given in Table 6. For brevity, only the ensemble average values are shown.

On average, a reduction of 53.51% is obtained using the IS system. Now, the effect of combining this system with the base isolation system is investigated. The results are given in the next section.

7.4. Combination of the IS system with the base isolation system

This part of the study investigates the effectiveness of combining the proposed IS system with the base isolation system. For this purpose, parameters of the IS system and those of the base isolators are simultaneously optimized by GA optimizer using the Pareto-optimal solutions (IS-BS-GA system). Again, for brevity, only the results of the ensemble average responses are shown in Table 7. As seen in the table, this newly proposed system is not only much more effective in reducing the building responses, it also brings the displacement of the base isolation system into a reasonable range. In this case, the ensemble average reduction ratio for the building's top story horizontal displacement response is about 82.1%, which is around 27%

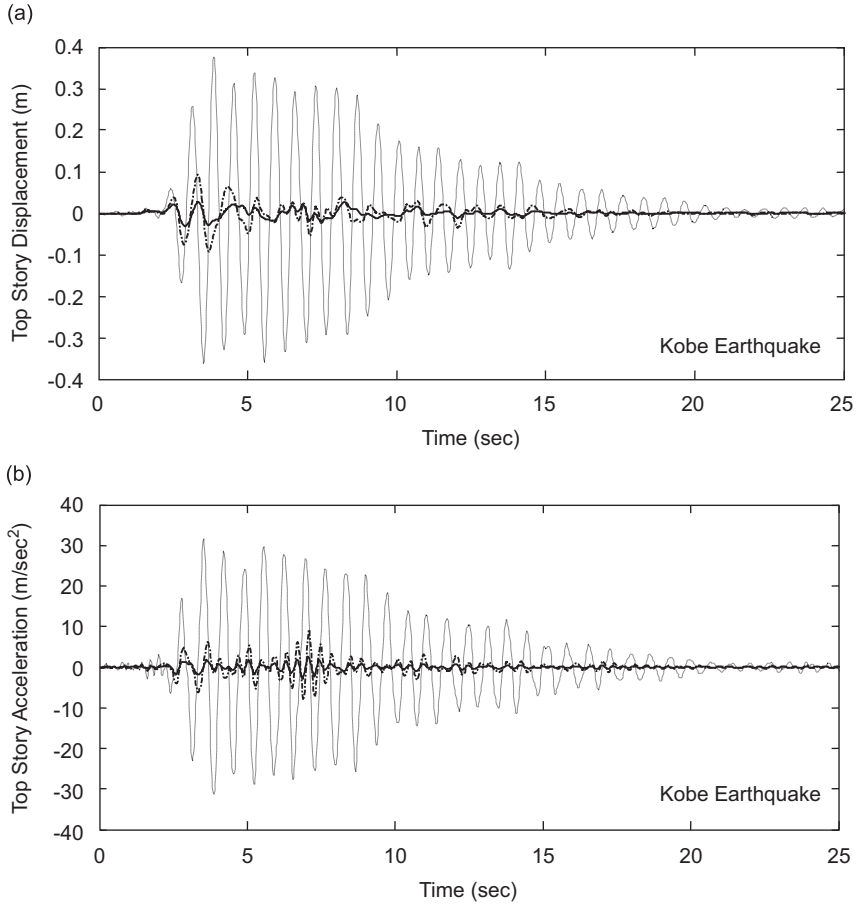

Fig. 14. Comparison of the effectiveness of the new, proposed, combined IS-BS-GA system with the linear base-isolation system with parameters optimized by GA: (a) horizontal displacement response and (b) acceleration response (——— non-isolated, -·-·-·- optimized by GA, and ——— IS-BS-GA).

greater than that of the linear base isolation system. For this system, the optimal IS-system parameter values and those of the base isolation system are:

$$m_0 = 0.78, \quad k_0 = 0.02, \quad \xi_b = 0.26, \quad m_{d0} = 0.93, \quad k_{d0} = 0.66.$$

For further comparison, time-histories of the building's top-story horizontal displacement and acceleration responses for the Kobe earthquake are shown in Fig. 14a and b, respectively. From the figures, the newly proposed IS-BS-GA system is seen to be much more effective than the other systems.

8. Conclusions

In the present paper, multi-objective optimization of the dynamic response of base-isolated tall building structures is studied. The isolated building is modeled as a 2-D, planar-shear frame with one lateral degree of freedom at each story level. Elastomeric bearing supports are considered as one additional degree of freedom with three unknown parameters: base mass, stiffness, and damping ratio. In order to calculate the building response, the governing equations of motion of the system are solved in state-space. The building's top story horizontal displacement and that of the base isolation system are considered the objective functions to be simultaneously minimized. The base isolators' mass, stiffness, and damping ratio are evaluated using GAs which take into account the linear and nonlinear behaviors of the isolator bearings. For this purpose, a fast and elitist NSGA-II approach is used to find a set of Pareto-optimal solutions.

Moreover, an IS system is proposed as a new method to simultaneously reduce both the building's dynamic response and that of the base isolation system. In this new method, the independent story is considered to lie between the $(i-1)$th and $(i+1)$th stories, without having any connection to the $(i+1)$th story. In fact, this system works as a big TMD system without using any of the additional damping or stiffness devices needed in ordinary TMD systems, except for those of the structure itself. Either one full story of the building or even a part of one story can be considered the IS system.

For a numerical example, a realistic ten-story building, located in Mashhad, Iran, was chosen. From the results of the numerical studies, it is found that:

1. Multi-objective optimization using the NSGA-II approach is a powerful method to design the parameters of the base isolators to make the isolation system more effective.
2. By calculating the parameters of the linear base-isolation system using GAs, a reduction of 64.5% is obtained for the ensemble average value (calculated for 18 worldwide earthquakes) of the building's top story horizontal displacement response.
3. By considering the nonlinearity of the lead-rubber bearings and optimizing their parameters using GAs, further reduction can be obtained for the building's top story horizontal displacement. However, due to the lead-rubber bearings' plastic deformation, the horizontal displacement of the base system increases.
4. In order to overcome the drawback of the bilinear isolators mentioned directly above, a new "IS" system is proposed. By combining this new system with the linear base-isolation system, the horizontal displacement is reduced by 82.1% for the building's top story, while the base displacement also remains in a reasonable range.

References

[1] C. Alhan, H. Gavin, A parametric study of linear and non linear passively damped seismic isolation system for buildings, *Engineering Structures* 24 (2004) 485–497.
[2] V.A. Matsagar, R.S. Jangid, Seismic response of base-isolated structures during impact with adjacent structures, *Engineering Structures* 25 (2003) 1311–1323.
[3] V.A. Matsagar, R.S. Jangid, Influence of isolator characteristics on the response of base-isolated structures, *Engineering Structures* 26 (2004) 1735–1749.
[4] Y.Y. Wu, B. Samali, Shake table testing of a base isolated model, *Engineering Structures* 24 (2002) 1203–1215.
[5] Uniform Building Code, International Conference of Building Officials, 1994 Edition.
[6] R.S. Rosenberg, Simulation of Genetic Populations with Biochemical Properties, PhD Thesis, University of Michigan, Ann Harbor, MI, 1967.

[7] J.D. Schaffer, Multiple objective optimization with vector evaluated genetic algorithms, in: J.J. Grefenstette (Ed.), *Proceedings of the First International Conference on Genetic Algorithms and their Applications*, Lawrence Erlbaum, London, 1985, pp. 93–100.
[8] C.M. Fonseca, P.J. Fleming, Genetic algorithms for multi-objective optimization: formulation, discussion and generalization, in: S. Forrest (Ed.), *Proceedings of the Fifth International Conference on Genetic Algorithms*, Morgan Kaufmann, San Mateo, CA, 1993, pp. 416–423.
[9] N. Srinivas, K. Deb, Multi-objective optimization using nondominated sorting in genetic algorithms, *Evolutionary Computation* 2 (3) (1994) 221–248.
[10] E. Zitzler, L. Thiele, *An evolutionary algorithm for multi-objective optimization: the strength pareto approach, Technical Report 43*, Computer Engineering and Federal Institute of Technology, Zurich, 1998.
[11] J. Knowles, D. Corne, The Pareto archived evolution strategy: a new baseline algorithm for multi-objective optimization, *Proceedings of the 1999 Congress on Evolutionary Computation*, IEEE Service Center, Piscataway, NJ, 1999, pp. 98–105.
[12] F. Naeim, J.M. Kelly, *Design of Seismic Isolated Structures, Earthquake Resistant Design*, United States of America, 1999.
[13] T.E. Kelly, *Base Isolation of Structures: Design Guidelines*, Holmes Consulting group Ltd., 2001 Revision 0.
[14] K. Deb, S. Agrawal, A. Pratap, T. Meyarivan, A fast and elitist multi-objective genetic algorithm: NSGA-II, *IEEE Transactions on Evolutionary Computation* 6 (2002) 182–197.
[15] R.I. Skinner, J.M. Kelly, A.J. Heine, Hysteretic damper for earthquake resistant structures, *Earthquake Engineering and Structural Dynamics* 3 (1975) 287.
[16] W.H. Robinson, Lead rubber hysteretic bearing suitable for protecting structures during earthquakes, *Earthquake Engineering and Structural Dynamics* 10 (1982) 593–604.
[17] J. Rodellar, V. Manosa, A robust tendon control schema for a class of cable-stayed structures, *Proceeding of the Third Conference on Structural Control*, Vol. 3, Como, Italy, 2003, pp. 184–190.
[18] M. Gen, R. Cheng, *Genetic Algorithms and Engineering Design*, Wiley, New York, 1997.
[19] Y.J. Kim, J. Ghaboussi, A new method of reduced order feedback control using genetic algorithms, *Earthquake Engineering and Structural Dynamics* 28 (1999) 193–212.
[20] C.A. Coello, A.D. Christiansen, Multi-objective optimization of trusses using genetic algorithms, *Computers & Structures* 75 (2000) 647–660.
[21] A. Osyczka, Multicriteria optimization for engineering design, in: J.S. Gero (Ed.), *Design Optimization*, New York, Academic Press, 1985.
[22] K. Deb, H. Gupta, Introducing robustness in multi-objective optimization, Technical Report (KanGAL Report No. 2004016), Department of Mechanical Engineering, Indian Institute of Technology, Kanpur, India, 2004.
[23] J. Branke, Creating robust solutions by means of an evolutionary algorithm, *Parallel Problem Solving from Nature* (1998) 119–128.
[24] Y. Jin, B. Sendhoff, Trade-off between performance and robustness: an evolutionary multi-objective approach, *EMO2003*, 2003, pp. 237–251.